

Biased reorientation in the chemotaxis of peritrichous bacteria *Salmonella enterica* serovar Typhimurium

Tonau Nakai,^{1,2,*} Taishi Ando,¹ and Tomonobu Goto^{1,2}

¹Department of Mechanical and Aerospace Engineering, Graduate School of Engineering and ²Advanced Mechanical and Electronic System Research Center, Faculty of Engineering, Tottori University, Tottori, Tottori, Japan

ABSTRACT Many kinds of peritrichous bacteria that repeat runs and tumbles by using multiple flagella exhibit chemotaxis by sensing a difference in the concentration of the attractant or repellent between two adjacent time points. If a cell senses that the concentration of an attractant has increased, their flagellar motors decrease the switching frequency from counterclockwise to clockwise direction of rotation, which causes a longer run in swimming up the concentration gradient than swimming down. We investigated the turn angle in tumbles of peritrichous bacteria swimming across the concentration gradient of a chemoattractant because the change in the switching frequency in the rotational direction may affect the way tumbles. We tracked several hundreds of runs and tumbles of single cells of *Salmonella enterica* serovar Typhimurium in the concentration gradient of L-serine and found that the turn angle depends on the concentration gradient that the cell senses just before the tumble. The turn angle is biased toward a smaller value when the cells swim up the concentration gradient, whereas the distribution of the angle is almost uniform (random direction) when the cells swim down the gradient. The effect of the observed bias in the turn angle on the degree of chemotaxis was investigated by random walk simulation. In the concentration field where attractants diffuse concentrically from the point source, we found that this angular distribution clearly affects the reduction of the mean-square displacement of the cell that has started at the attractant source, that is, the bias in the turn angle distribution contributes to chemotaxis in peritrichous bacteria.

SIGNIFICANCE We found another aspect in the chemotactic behavior of peritrichous bacteria. Chemotactic behaviors in peritrichous bacteria were predicted to be observed at the turn angles during tumbles motion as well as at the duration of runs; smaller changes in the swimming direction of cells swimming up the attractant's gradient can be observed. This behavior is appropriate because the nature of bacterial chemotaxis changes the switching rate of the rotational direction of the flagellar motors according to the environment. Cells swimming upward reduce the turn angle by switching fewer flagellar motors to loosen flagellar filaments from the bundle during tumbles. We have shown that this prediction is correct.

INTRODUCTION

Many kinds of bacteria exhibit chemotaxis; the cells accumulate around a favorable substance (attractant) or recede from an unfavorable one (repellent). The mechanism of chemotaxis has been intensely studied in peritrichous bacteria (1–3), such as *Escherichia coli* and *Salmonella enterica*, which have multiple flagella. Cells swim by rotating the helical flagella with the help of flagellar motors located at the proximal ends of the flagella. When each motor rotates counterclockwise (CCW), when observed from the distal

end of the flagellum to the motor, the flagella form a bundle, and the cell propels itself (run). When the rotational direction of the motors switches to clockwise (CW), the corresponding flagella are released from the bundle and the swimming direction of the cell changes (tumble) (4–6). For *E. coli* cells, the mean time durations of run and tumble movements are ~1 and 0.1 s, respectively (7).

Cells exhibit chemotaxis upon sensing a difference in the concentration of the attractant or repellent between two adjacent time points (8,9). If a cell senses that the concentration of an attractant has increased, their flagellar motors decrease the switching frequency from CCW to CW direction of rotation, which causes a longer run in swimming up the concentration gradient than swimming down. Although a cell cannot move in a particular direction after exhibiting tumble motion

Submitted November 9, 2020, and accepted for publication April 26, 2021.

*Correspondence: nakai@tottori-u.ac.jp

Editor: Pablo Iglesias.

<https://doi.org/10.1016/j.bpj.2021.04.033>

© 2021 Biophysical Society.

This is an open access article under the CC BY license (<http://creativecommons.org/licenses/by/4.0/>).



or situate itself at the optimal position (with the maximal concentration of the attractant), the cell can remain at region where the concentration of the attractant is comparatively high. Longer runs toward the attractant have been observed in *E. coli* (7,9) and *S. enterica* (10).

Although the characteristic behavior of the chemotaxis of peritrichous bacteria is the biased random walk, the bias in the turn angle distribution, subject of this article, was rarely referred to in the review articles in this field. The dependence of the duration of runs on the concentration gradient of the attractant has been mainly described (1,11–13). In a review article by Mitchell and Kogure (14), various kind of biases in the reorientation was shown: tumbling, reversing, steering, and so on. Berg and Brown (7) reported that the turn angle of *E. coli* is not completely random but biased to the forward hemisphere. However, the difference in the turn angle distribution between up and down the gradient was not described in these articles. Recently, Sourjik and Wingreen (8) predicted that chemotaxis, in peritrichous bacteria, can be observed at the turn angles during tumbles. The authors in the article refer to smaller changes in the swimming direction of cells swimming up the attractant's gradient. This prediction is based on an observational study with regard to flagellar filaments in *E. coli* cells during tumble, which indicated that the turn angle reduces when fewer filaments are released during a tumble (15). *E. coli* cells have five to six flagella on an average, and the corresponding flagellar motors can independently switch the direction of rotation (16). The number of flagella released during tumble varies and can decrease when the switching from CCW to CW direction of rotation is suppressed when a chemoattractant is sensed. Turner et al. (15) also demonstrated that the turn angle distribution is uniform (random direction) when many flagella are released during a tumble. The apparent influence of this change in the turn angle distribution on the chemotactic behavior has been confirmed by performing numerical simulation (17). Experimentally, Saragosti et al. (18) demonstrated that the drift velocity of *E. coli* cells in the attractant gradient has to be estimated by biases in the distribution of the turn angles as well as the duration of runs.

Our aim in this study was to demonstrate that the turn angle distribution depends on the swimming direction (up or down the concentration gradient). We observed the chemotactic behavior of a single cell for a long time to directly relate the cell's movement with the degree of accumulation. Short-time observation of many cells would result in obtaining ambiguous information about characteristic motions because of difference in the swimming motion of each cell; hence, we chose to observe for a longer period of time.

MATERIALS AND METHODS

A strain of peritrichous bacteria, *S. enterica* serovar Typhimurium (*S. Typhimurium*) SJW1103, was used. Cells were cultured in 3 mL of Luria-Bertani medium (1% polypeptone, 0.5% yeast extract, and 0.5% sodium chloride)

overnight at 30°C. Then, 0.1 mL of the bacterial suspension was added to 3 mL of the motility buffer (pH 7.0, 10 mM KH₂PO₄, 0.1 mM EDTA, and 10 mM sodium lactate) and incubated for 3 h at 30°C. The solution was centrifuged for 1 min at 10,000 rpm (CHIBITAN-II; Merck, Tokyo, Japan). The supernatant 0.9 mL was removed, and same amount of buffer was added to remove the culture medium for the detection of an attractant. The size of the cells was 1–2 μm in length and 0.6–0.8 μm in width.

Capillary assay was performed, in which cells were made to accumulate around the tip of a capillary filled with an attractant (same as that followed by authors in (10)). A capillary was made by pulling a glass tube with a filament (GD-1; Narishige, Tokyo, Japan) using a puller (PC-10; Narishige). The inner diameter of the tip was 3–4 μm. L-serine (molecular weight (MW) = 105; Wako Pure Chemical Industries, Osaka, Japan) was used as the attractant. To prevent the flow as a result of capillary force, the attractant solution was jellified with agar. One molar L-serine with 0.3% agar (Agarose L; Wako Pure Chemical Industries), dissolved in the motility buffer, was heated with the help of a hot plate at 80°C and then aspirated into the capillary. Then, the outer surface of the capillary was washed with distilled water. As shown in Fig. 1, the capillary and the bacterial suspension were inserted between the slide glass (S7224, 76 mm × 26 mm, thickness 1.2–1.5 mm; Matsunami Glass, Osaka, Japan) and cover glass (18 mm × 18 mm, thickness 0.13–0.17 mm; Matsunami Glass). Bacteria were aspirated using a microinjection (IM-6; Narishige) with a capillary (inner diameter of ~100 μm) and poured into the preparation. Then, 150 μL of buffer was added. To prevent convection as a result of evaporation, the edge of the cover glass was sealed with petroleum jelly. The thickness of the suspension was ~300 μm.

Cells accumulating around an attractant were observed using an inverted microscope (IX71; Olympus, Tokyo, Japan) with an objective lens (LUCPLFLN40XPH, NA = 0.60; Olympus). The capillary tip was set at the center of the view. Images were recorded using a digital camera (DP27; Olympus) at 30 fps with a resolution of 1216 × 960 pixels (corresponding to the field of view of 280 × 220 μm). Images were analyzed using a tracking software (DippMotionPro; Ditect, Tokyo, Japan) and the two-dimensional trajectories of cells were measured.

As the flagella were not visible in bright field observation, the time of tumble was judged from the change in both the swimming direction and the swimming speed. Fig. 2 shows the change in the bacterial swimming speed and the swimming direction (up or down the concentration gradient of the attractant), together with the trajectory of the cell. Berg and Brown (7) also determined the time of tumble using this method. Although our data are two-dimensional projections of three-dimensional motion, a decrease in the swimming speed is seen at the time of tumble motion.

The characteristic time of the diffusion of L-serine can be roughly estimated from the diffusion constant D . In aqueous solution, the diffusion constant D is of the order 10⁻⁹ m²/s at 20°C. Consequently, the time τ required for L-serine molecules at the capillary tip to diffuse outside of the view can be approximately estimated using the below equation:

$$\tau \sim \frac{(100 \mu\text{m})^2}{D} = 10 \text{ s} . \quad (1)$$

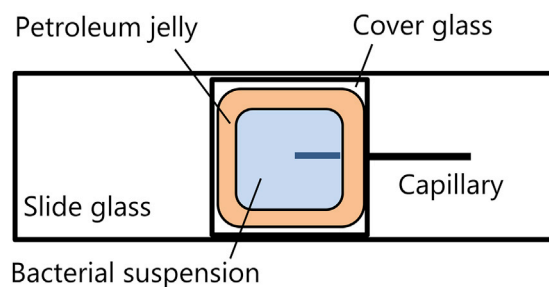


FIGURE 1 Top view of the prepared slide for observation of the bacterial chemotaxis. To see this figure in color, go online.

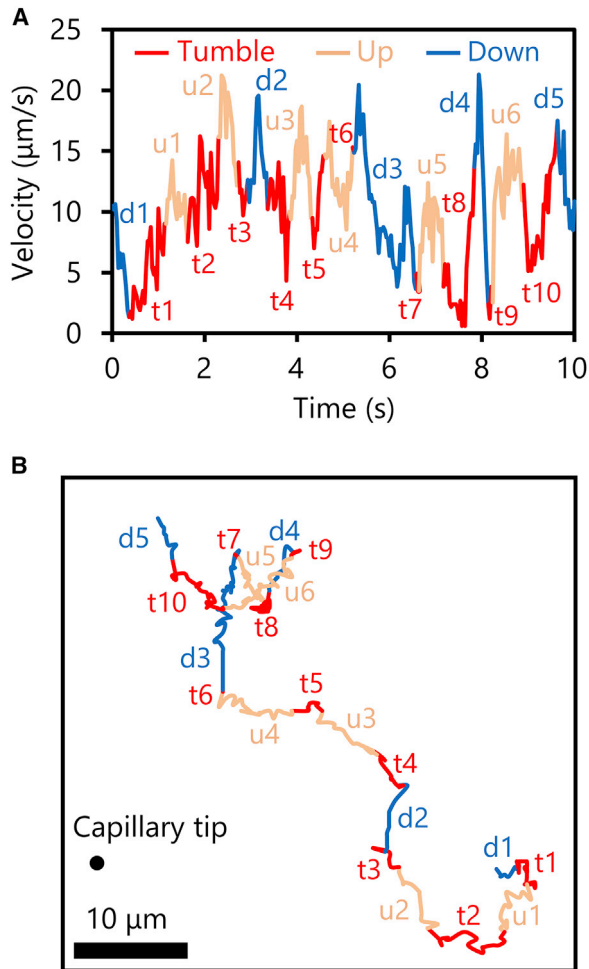


FIGURE 2 Motion of runs and tumbles of a *S. Typhimurium* cell around the capillary filled with L-serine. (A) Relationship between the time of tumble and the decrease in the swimming velocity. (B) Trajectory of the cell corresponding to (A). The terms “Up” and “Down” mean that the cell swims up and down the concentration gradient of the attractant, respectively. To see this figure in color, go online.

Hence this estimation implies that the concentration field of serine could be formed in several tens of seconds. To check the stable and concentric concentration field in the capillary assay mentioned, a fluorescent dye was used instead of L-serine. A capillary filled with 10 mM fluorescein (MW = 332; Wako Pure Chemical Industries) was observed using a laser scanning confocal microscope (FV10i; Olympus) with a 10 \times objective lens. As shown in Fig. S1, the fluorescence distribution around the tip was almost concentric, which continued for at least 20 min. Thus, a similar concentration gradient of an attractant is also assumed in the observation of the chemotactic behavior of cells (within 15 min).

RESULTS

Trajectory of the trapped cell around an attractant

We analyzed 23 cells, the tracking time of which exceeded 30 s. Fig. 3 A shows an example of a swimming trajectory (sample II in Fig. 3 B). The cell remains within 100 μm from the source of attractant. Whether this movement ex-

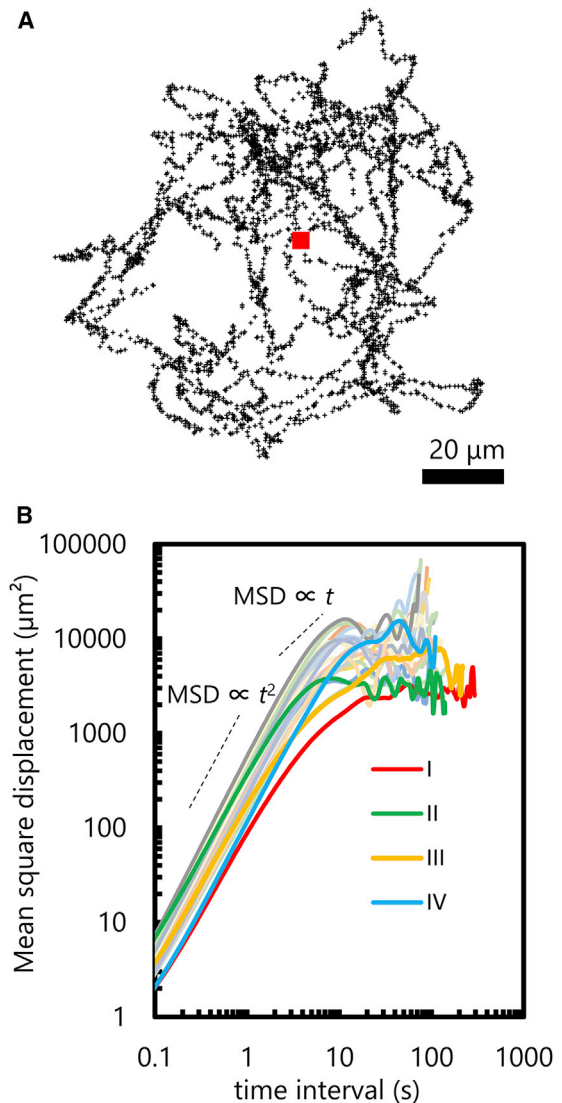


FIGURE 3 A single cell's behavior around attractant source (L-serine). (A) Trajectory for sample II. The red square represents the position of the capillary tip. (B) MSD of 23 cells. Thick lines named I–IV correspond to cells with longer tracking time, analyzed in detail in Figs. 4, 5, 6, and 7. To see this figure in color, go online.

hibits chemotaxis or the movement is only a random walk can be determined by calculating the mean-square displacement (MSD). Fig. 3 B shows MSD of 23 cells, in which the cells with longer tracking time are highlighted as samples I–IV. As shown in Fig. 3 B, the MSDs of the cells reach a plateau in the time region 10–100 s, indicating that the cells are attracted to the capillary tip. Without an attractant, the MSD should increase linearly with time.

Duration of runs

The duration of runs, the time between two adjacent tumbles, is one of the characteristics of bacterial chemotaxis, as reported in previous studies (7,10). In Fig. 4 A, the duration of

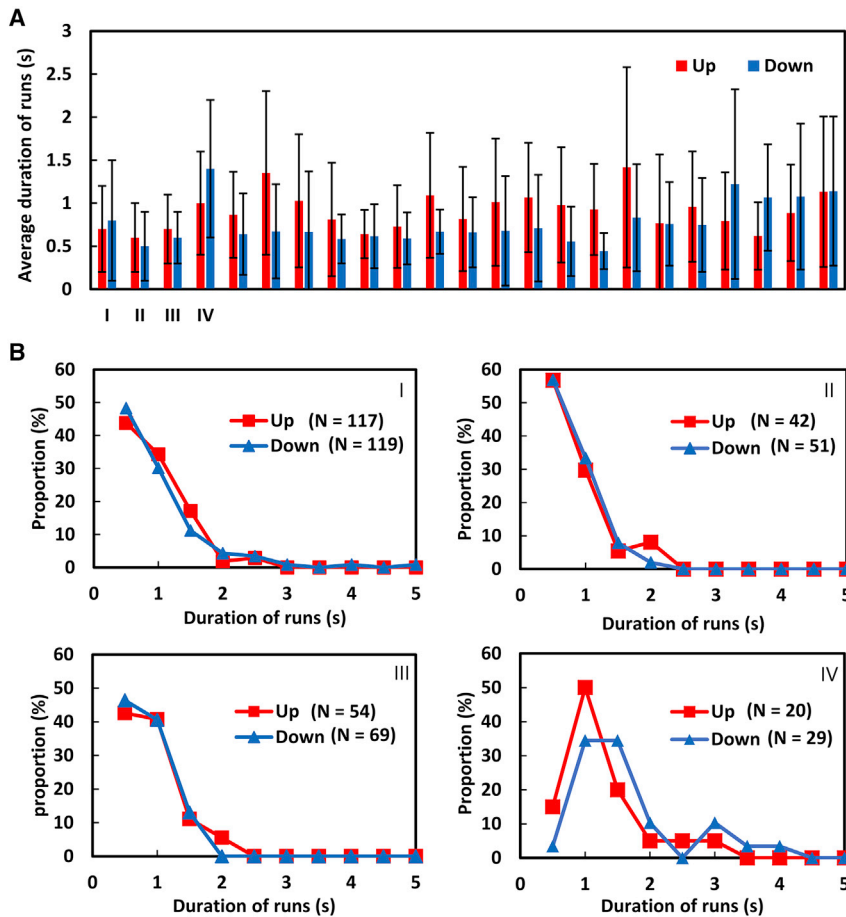


FIGURE 4 Duration of runs of a single cell around an attractant. (A) Comparison between swimming up and down the concentration gradient of the chemoattractant for 23 cells. (B) Distribution of runs in samples I–IV. The vertical axis denotes the percentage of total runs for each cell. To see this figure in color, go online.

runs for 23 cells is shown, where runs are split, that is, with regard to swimming up and down the gradient. Data for the runs passing by the capillary tip ($\sim 20\%$ of total runs) are not shown. Although the average durations of runs “up” is slightly longer than “down” as a general trend, some cells do not exhibit difference between up and down (for example, samples I–IV); this is not completely in agreement with previous studies, in which the duration of runs was measured by using many bacterial cells (7,10), where duration for “up” movement is ~ 1.5 times longer than the duration of “down” movement. In Fig. 4 B, the distribution of the duration of runs for “up” and “down” is shown for samples I–IV. The vertical axis denotes the percentage of each “up” and “down” motion for each cell. The short run (0–1 s) seems less frequent in “up” movement, but the shape of the distribution and peak position are almost the same. Long runs (2–3 s) are seen in both “up” and “down” movements especially in sample IV, which may obscure the difference in the average values (around 1 s).

Turn angle

The dependence of the swimming direction on the turning angle has been elucidated. As shown in Fig. 5 A, the turn angle θ and the swimming direction φ are defined as the

change in the swimming direction between two adjacent runs and the orientation angle relative to the capillary tip, respectively. In Fig. 5 B, a plot of θ and φ for all 268 tumbles in sample I is shown. The orientation angle φ is less than 90° for “up” moving cells and larger than 90° for “down” moving cells. The turn angle θ is distributed uniformly when $\varphi > 90^\circ$, whereas the distribution of θ is biased to a smaller angle when $\varphi < 90^\circ$. This indicates that cells approaching the attractant source have a smaller average turn angle than receding cells. The mean values of the turn angles are different between “up” and “down” movements in the t -test with a significance level of 5%. The φ - θ plot of all the 23 cells is also shown in Fig. 5 B, where the difference in the turn angle θ is apparent between “up” and “down.”

As shown in Fig. 5 C, the bias in the single cell can be clearly visualized by plotting the cumulative probability of θ for “up” ($\varphi < 90^\circ$) and “down” ($\varphi > 90^\circ$). The dashed straight line denotes that the turn angle θ has random distribution; θ is observed with equal probability at any angle. In samples I–IV, “down” is almost random and “up” has a plot above “down,” indicating that the directional change during the tumble after swimming up the gradient tends to be smaller. This tendency in the angle distribution was the same in the three-dimensional measurement using a

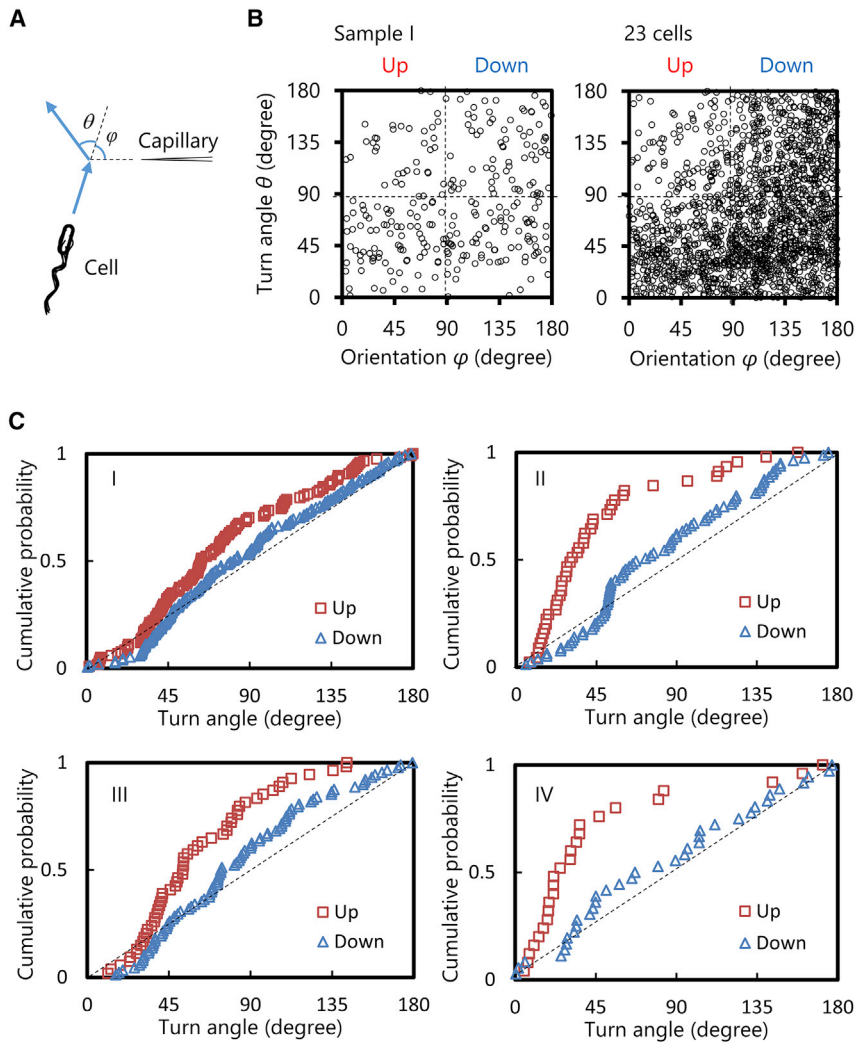


FIGURE 5 Turn angle distribution in a single cell. (A) Definition of the directional change θ and the orientation φ . (B) θ - φ plot for sample I and 23 cells. (C) Cumulative probability of the turn angle. To see this figure in color, go online.

piezoelectric-driven objective lens (see the [Supporting materials and methods](#)).

Biased random walk simulation

The effect of the observed bias in the turn angle on the degree of accumulation was investigated by numerical simulation. Goto et al. developed a mathematical model for bacterial chemotaxis based on the biased random walk (10,19) in which the cell changes the tumble frequency depending on the moving direction of the adjacent steps. In this subsection, we consider the bias in the turn angle in addition to the change in the tumble frequency.

We have herein provided the details of the mathematical model. As schematized in Fig. 6 A, an attractant source is at the origin, and a concentric concentration field because of diffusion is assumed. The rules for the modeled cells are as follows:

- 1) Cells migrate a constant distance Δr during a unit time step Δt .

- 2) When the cell has moved toward the direction in which the concentration of an attractant increases, that is, toward the source of an attractant, the cell moves in the same direction as the previous time step with the probability α (see Fig. 6 A). Alternatively, the cell changes its direction with probability $1 - \alpha$, in which the direction in the next step follows the observed distribution “up” (Fig. 6 B).
- 3) A cell changes its direction in the random direction when the cell has moved toward the direction where the concentration decreases. The direction in the next step is determined randomly, reflecting the distribution “down” as in Fig. 5 C.

It must be noted that the swimming of cells up or down the gradient is dependent on the cell, and the cells do not sense how large the concentration gradient is. The parameter α ($0 \leq \alpha \leq 1$) denotes the intensity of the chemotaxis; $\alpha = 1$ is the maximal intensity and $\alpha = 0$ is the minimum, that is, the random walk without biases. As for the turn angles, a simplified cumulative distribution of the observation was

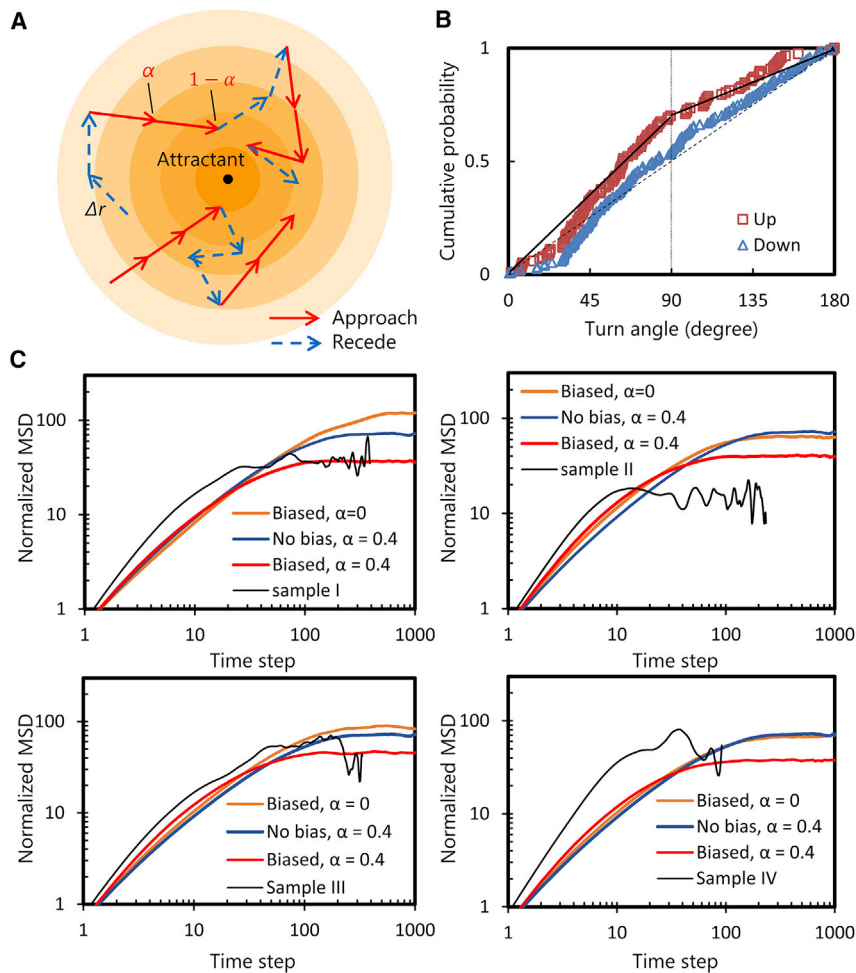


FIGURE 6 Biased random walk simulation of a swimming cell in the concentration gradient of a chemoattractant. (A) Scheme of the simulation model. Each cell migrates a constant distance Δr in a unit time step, corresponding to each arrow. Cells receding from the attractant source always tumble, whereas cells approaching the attractant continue run with the probability α . (B) Modeling the difference in the turn angle between “up” and “down” for sample I. (C) Calculated MSD together with the observed one. Note that the term “Biased” and “No bias” in the graphs mean the bias only in the turn angle (not in the tumble frequency). To see this figure in color, go online.

applied, as shown in Fig. 6 B. In the figure, the thick solid line represents a distribution for a cell that moved “up,” where the folding point at 90° implies that the probability that turn angle becomes smaller than 90° is higher. The turn angle for a cell that moved “down” is assumed to be a random value, as represented by a dashed line in the figure. Although the cumulative distribution is based on the two-dimensional measurement, we have confirmed the validity of the distribution by conducting three-dimensional measurement of turn angles. For details, see the [Supporting materials and methods](#).

Fig. 6 C shows the calculated MSDs together with the observed ones. For comparison with the two-dimensional microscopic observation, MSD was calculated from the two-dimensionally projected trajectory. The MSD and time interval in the observation were made dimensionless by the average values of run length and duration of runs, respectively. The condition corresponding to the observation is “Biased, $\alpha = 0$.” To compare the chemotaxis intensity in the case where cells change the duration of runs and have no bias in the turn angle distribution, calculation results with “No bias, $\alpha = 0.4$ ” is also shown, which was the estimated α in a previous study (10). Because both MSDs reach a plateau of same

height, the observed bias in the turn angle distribution contributes to the bacterial chemotaxis.

As for the height of the plateau, the observed MSD is several times smaller than “Biased, $\alpha = 0$,” especially in samples I and II. Considering $\alpha = 0.4$, together with the biased angle distribution (“Biased, $\alpha = 0.4$ ” in the graph), the plateau value of MSD becomes almost the same. However, the time interval until reaching the plateau is much smaller in the observation especially in sample IV, and the slope of the MSD in the region where the time interval is of 1–10 steps is steeper in the observation. Thus, even in the calculation model considering the angle distribution and α , we were not able to reproduce the observed result; possible reasons will be described in the next section.

DISCUSSION

Difference in MSD between observation and simulation

From Fig. 6 C, it can be seen that the observed bias in the turning angle affects the bacterial behavior around an

attractant. However, some parts of the calculated MSD curve are quantitatively not in correspondence with the observation results, the cause of which is discussed in this subsection.

As can be seen from Fig. 4 B, long runs of over 2 s are observed in both “up” and “down” movements; this could result in the slope of the observed MSD being steeper in the short-time region than in the simulation (Fig. 6 C). For the reason that the average duration of runs (~ 1 s) is adopted as the time step in the simulation, these long runs correspond to several time steps. Therefore, the slope of the MSD in the observation is almost 2 (ballistic) in the region of several time steps, whereas the slope is almost 1 (diffusive) in the simulation.

These long runs also affect the average value of the duration of runs: no difference between “up” and “down” that leads to the higher plateau of MSD in the simulation (“biased, $\alpha = 0$ ” in Fig. 6 C). In Fig. 4 B, runs of 1 s have a larger ratio for “Down.” Therefore, it is considered that α would have a positive value more than 0. However, with regard to the average duration of runs including these long runs, the upward runs may not be longer than downward runs (Fig. 4 A).

One of the reasons for these long runs could be recovery from the adaptive state to the chemoattractant. Adaptation means that the bacteria become accustomed to the environment with the attractant and cannot detect the attractant unless bacterial cells move to a higher concentration. If the environment changes from no attractant to a uniform concentration (no concentration gradient) of the attractant, tumble frequency is reduced for the first minute but then changes to the same frequency as the environment without the attractant (9). In our experiment, it is possible that the bacteria migrated to a low-concentration region of the attractant (far from the capillary tip) and recovered from the adaptive state, which caused long runs independent of the swimming direction.

Duration of tumbles: guessing the number of flagellar filaments loosen

Although flagella were not observed in our experiment, the number of flagella (corresponding to the turn angle) loosened during the tumble can be inferred from the duration of the tumble. Switching of the rotational direction of each flagellar motor occurs independently; hence, in a tumble with multiple flagella loosened, switching of multiple flagellar motors occurs within a short time, and the observed duration of the tumble is expected to be long. In Fig. 7, the distribution of the duration of tumbles for each swimming direction for four each cell is shown. The vertical axis is the ratio that becomes 1 when integrating only “up” or “down” movements. There seems a trend that a large number of short-time tumble motions (~ 0.1 s) was observed in “up” in sample II, implying that the number of flagella loosened during tumble tends to be small in “up.” However, this trend was not significant in samples I, III, and IV at 5% level of *t*-test. For further discussion, direct observation of the flagellar filaments is necessary to precisely measure the duration of tumbles.

CONCLUSIONS

We investigated the turn angle in tumbles of peritrichous bacteria swimming across the concentration gradient of a chemoattractant. As predicted in (8,13,14), we found that the turn angle depends on the concentration gradient that the cell senses just before the tumble. The turn angle is biased toward a smaller value when the cells swim up the concentration gradient, whereas the distribution of the angle is almost uniform (random direction) when the cells swim down the gradient; this behavior is appropriate because the nature of bacterial chemotaxis changes the switching rate of the rotational direction of the flagellar motors

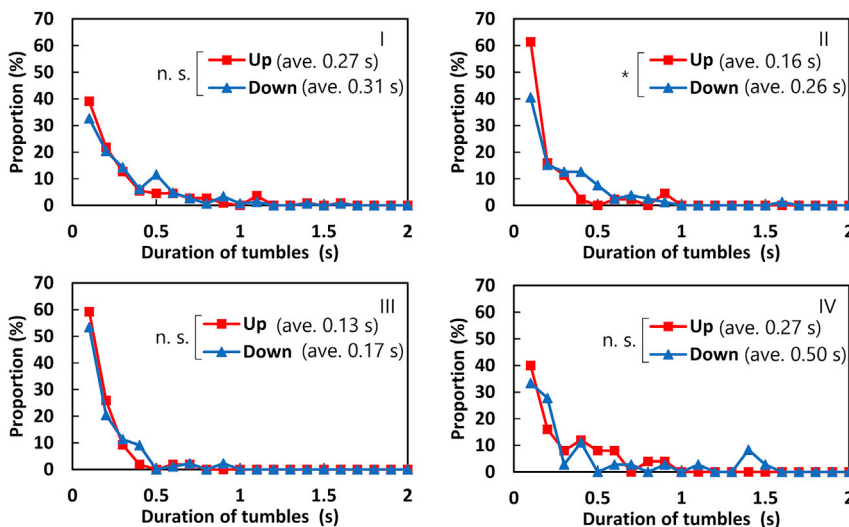


FIGURE 7 Distribution of the duration of the tumbles for samples I–IV. The asterisk in sample II means that the distributions are significantly different at 5% level of *t*-test. To see this figure in color, go online.

according to the environment. Cells swimming upward reduce the turn angle by loosening fewer flagellar filaments from the bundle during tumbles, resulting in accumulation at higher concentrations of the chemoattractant. The effect of the observed bias in the turn angle on the degree of chemotaxis was investigated by random walk simulation. In the concentration field where attractants diffuse concentrically from the point source, we found that this angular distribution clearly affects the reduction of the MSD of the cell, that is, the bias in the turn angle distribution contributes to chemotaxis in peritrichous bacteria.

SUPPORTING MATERIAL

Supporting material can be found online at <https://doi.org/10.1016/j.bpj.2021.04.033>.

AUTHOR CONTRIBUTIONS

T.N. and T.G. designed research. T.A. performed experiments and analyzed data. T.N. wrote the article.

ACKNOWLEDGMENTS

This work was supported by Japan Society for the Promotion of Science KAKENHI grant numbers JP18K03950 and 19K04193.

REFERENCES

- Berg, H. C. 2004. *E. coli in Motion*. Springer-Verlag, New York.
- Krembel, A. K., S. Neumann, and V. Sourjik. 2015. Universal response-adaptation relation in bacterial chemotaxis. *J. Bacteriol.* 197:307–313.
- Neumann, S., N. Vladimirov, ..., V. Sourjik. 2014. Imprecision of adaptation in *Escherichia coli* chemotaxis. *PLoS One.* 9:e84904.
- Berg, H. C. 1974. Dynamic properties of bacterial flagellar motors. *Nature.* 249:77–79.
- Silverman, M., and M. Simon. 1974. Flagellar rotation and the mechanism of bacterial motility. *Nature.* 249:73–74.
- Berg, H. C. 2003. The rotary motor of bacterial flagella. *Annu. Rev. Biochem.* 72:19–54.
- Berg, H. C., and D. A. Brown. 1972. Chemotaxis in *Escherichia coli* analysed by three-dimensional tracking. *Nature.* 239:500–504.
- Sourjik, V., and N. S. Wingreen. 2012. Responding to chemical gradients: bacterial chemotaxis. *Curr. Opin. Cell Biol.* 24:262–268.
- Macnab, R. M., and D. E. Koshland, Jr. 1972. The gradient-sensing mechanism in bacterial chemotaxis. *Proc. Natl. Acad. Sci. USA.* 69:2509–2512.
- Nakai, T., J. Yoshino, and T. Goto. 2019. Estimation of chemotaxis intensity of *Salmonella* cells by the capillary assay and biased random walk simulation. *J. Aero Aqua Bio-mech.* 8:63–68.
- Adler, J. 1975. Chemotaxis in bacteria. *Annu. Rev. Biochem.* 44:341–356.
- Vladimirov, N., and V. Sourjik. 2009. Chemotaxis: how bacteria use memory. *Biol. Chem.* 390:1097–1104.
- Karmakar, R. 2021. State of the art of bacterial chemotaxis. *J. Basic Microbiol.* 61:366–379.
- Mitchell, J. G., and K. Kogure. 2006. Bacterial motility: links to the environment and a driving force for microbial physics. *FEMS Microbiol. Ecol.* 55:3–16.
- Turner, L., W. S. Ryu, and H. C. Berg. 2000. Real-time imaging of fluorescent flagellar filaments. *J. Bacteriol.* 182:2793–2801.
- Ishihara, A., J. E. Segall, ..., H. C. Berg. 1983. Coordination of flagella on filamentous cells of *Escherichia coli*. *J. Bacteriol.* 155:228–237.
- Vladimirov, N., D. Lebiedz, and V. Sourjik. 2010. Predicted auxiliary navigation mechanism of peritrichously flagellated chemotactic bacteria. *PLoS Comput. Biol.* 6:e1000717.
- Saragosti, J., V. Calvez, ..., P. Silberzan. 2011. Directional persistence of chemotactic bacteria in a traveling concentration wave. *Proc. Natl. Acad. Sci. USA.* 108:16235–16240.
- Goto, T., and T. Nakai. 2016. Steady distribution of cells in a one-dimensional biased random walk model of bacterial chemotaxis. *J. Biomech. Sci. Eng.* 11:15–00587.